Article

Theoretical Study of the Oxygen Exchange in Uranyl Hydroxide. An Old Riddle Solved?

Grigory A. Shamov, and Georg Schreckenbach

J. Am. Chem. Soc., **2008**, 130 (41), 13735-13744 • DOI: 10.1021/ja804742f • Publication Date (Web): 23 September 2008

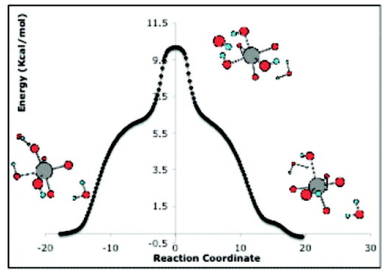

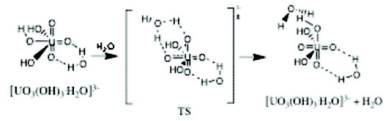

More About This Article

Additional resources and features associated with this article are available within the HTML version:

- Supporting Information
- Access to high resolution figures
- Links to articles and content related to this article
- Copyright permission to reproduce figures and/or text from this article

View the Full Text HTML

J|A|C|S
ARTICLES

Published on Web 09/23/2008

Theoretical Study of the Oxygen Exchange in Uranyl Hydroxide. An Old Riddle Solved?

Grigory A. Shamov and Georg Schreckenbach*

Department of Chemistry, University of Manitoba, Winnipeg, Manitoba, Canada, R3T 2N2

Received June 20, 2008; E-mail: schrecke@cc.umanitoba.ca

Abstract: A multistep mechanism for the experimentally observed oxygen exchange [*Inorg. Chem.* **1999**, *38*, 1456] of UO_2^{2+} cations in highly alkaline solutions is suggested and probed computationally. It involves an equilibrium between $[UO_2(OH)_4]^{2-}$ and $[UO_2(OH)_5]^{3-}$, followed by formation of the stable $[UO_3(OH)_3 \cdot H_2O]^{3-}$ intermediate that forms from $[UO_2(OH)_5]^{3-}$ through intramolecular water elimination. The $[UO_3(OH)_3 \cdot H_2O]^{3-}$ intermediate facilitates oxygen exchange through proton shuttling, retaining *trans*-uranyl structures throughout, without formation of the *cis*-uranyl intermediates proposed earliar. Alternative *cis*-uranyl pathways have been explored but were found to have activation energies that are too high. Relativistic density functional theory (DFT) has been applied to obtain geometries and vibrational frequencies of the different species (reactants, intermediates, transition states, products) and to calculate reaction paths. Two different relativistic methods were used: a scalar four-component all-electron relativistic method and the zeroeth-order regular approximation. Calculations were conducted for both gas phase and condensed phase, the latter treated using the COSMO continuum model. An activation energy of 12.5 kcal/mol is found in solution for the rate-determining step, the reaction of changing the four-coordinated uranyl hydroxide to the five-coordinated one. This compares favorably to the experimental value of 9.8 ± 0.7 kcal/mol. Activation energies of 7.8 and 5.1 kcal/mol are found for the hydrogen transfer between equatorial and axial oxygens through a water molecule in $[UO_3(OH)_3 \cdot H_2O]^{3-}$ in the gas phase and condensed phase, respectively. Contrary to previously proposed mechanisms that resulted in high activation barriers, we find energies that are low enough to facilitate the reaction at room temperature. For the activation energies, two approximate DFT methods, B3LYP and PBE, are compared. The differences in activation energies are only about 1−2 kcal/mol for these methods.

Introduction

The chemistry of the early actinide elements is important both for the nuclear industry and from the point of view of disposal and storage of nuclear waste and remediation of contaminated sites.[1] Experimental studies on actinide compounds are complicated by the radioactivity of these elements and the resulting nuclear waste problems. Moreover, in aqueous solution, there are often complicated equilibria involving multiple species such as monomers, dimers, trimers, etc.[1−3] Overall, there is room for theoretical investigations to provide complementary data, even though theoretical studies have their own complications that need to be considered.[4,5] These originate from the combination of electron−electron correlation including multiplet effects, relativity including spin−orbit, and medium (solvent) effects. Moreover, the large number of electrons results in simulations that are inherently large and challenging.

In the higher oxidation state of the actinide element (An^V, An^{VI}), the stable actinyl cations $AnO_2^{1+/2+}$ are often formed and are central to the (aqueous) chemistry of these elements accordingly. Uranyl hydrates and hydroxides can be considered to be the most simple and prototypical complexes in solution, and they have been investigated both experimentally and theoretically.[5−55] In this article, we will investigate the hydroxide complexes of uranyl(VI).

(1) Morss, L. R.; Edelstein, N. M.; Fuger, J.; Katz, J. J. *The Chemistry of the Actinide and Transactinide Elements*, 3rd ed.; Springer: Berlin, 2006.
(2) Baes, C. F.; Mesmer, R. E. *The Hydrolysis of Cations*. Wiley: New York, 1976.
(3) Clark, D. L.; Hobart, D. E.; Neu, M. P. *Chem. Rev.* **1995**, *95*, 25.
(4) Kaltsoyannis, N. *Chem. Soc. Rev.* **2003**, *32*, 9.
(5) Schreckenbach, G.; Hay, P. J.; Martin, R. L. *J. Comput. Chem.* **1999**, *20*, 70.
(6) Jones, L. H.; Penneman, R. A. *J. Chem. Phys.* **1953**, *21*, 542.
(7) Basile, L. J.; Sullivan, J. C.; Ferraro, J. R.; LaBonville, P. *Appl. Spectrosc.* **1974**, *28*, 142.
(8) Toth, L. M.; Begun, G. M. *J. Phys. Chem.* **1981**, *85*, 547.
(9) Madic, C.; Begun, G. M.; Hobart, D. E.; Hahn, R. L. *Inorg. Chem.* **1984**, *23*, 1914.
(10) Combes, J.-M.; Chisholm-Brause, C. J., Jr.; Parks, G. A.; Conradson, S. D.; Eller, P. G.; Triay, I. R.; Hobart, D. E.; Meijer, A. *Environ. Sci. Technol.* **1992**, *26*, 376.
(11) Allen, P. G.; Bucher, J. J.; Shuh, D. K.; Edelstein, N. M.; Reich, T. *Inorg. Chem.* **1997**, *36*, 4676.
(12) Bardin, N.; Rubini, P.; Madic, C. *Radiochim. Acta* **1998**, *83*, 189.
(13) Conradson, S. D. *Appl. Spectrosc.* **1998**, *52*, 252A.
(14) Wahlgren, U.; Moll, H.; Grenthe, I.; Schimmelpfennig, B.; Maron, L.; Vallet, V.; Gropen, O. *J. Phys. Chem. A* **1999**, *103*, 8257.
(15) Farkas, I.; Banyai, I.; Szabo, Z.; Wahlgren, U.; Grenthe, I. *Inorg. Chem.* **2000**, *39*, 799.
(16) Antonio, M. R.; Soderholm, L.; Williams, C. W.; Blaudeau, J. P.; Bursten, B. E. *Radiochim. Acta* **2001**, *89*, 17.
(17) Semon, L.; Boehme, C.; Billard, I.; Hennig, C.; Lutzenkirchen, K.; Reich, T.; Rossberg, A.; Rossini, I.; Wipff, G. *ChemPhysChem* **2001**, *2*, 591.
(18) Den Auwer, C.; Simoni, E.; Conradson, S.; Madic, C. *Eur. J. Inorg. Chem.* **2003**, 3843.

Experimental actinyl chemistry in solution is challenging because of the complex equilibria present and their pH dependence.[1] Whereas the chemistry of the uranyl(VI) ion under acidic conditions is relatively well-known,[1] there is less certainty regarding highly alkaline conditions that are particularly relevant to waste storage tanks. A major step in this field was achieved by the seminal work of Clark et al.[45] (published in 1999, though the majority of the data had been available since about 1997) who studied uranyl under highly alkaline conditions. A central feature of these investigations was the use of a bulky counterion that prevented precipitation of uranyl salts from solution. Among the major findings of this study were the following: solid-state (X-ray) and solution structure, vibrational spectroscopy, and establishment of a solution equilibrium between tetra- and penta-coordination in the equatorial plane, according to the following equation:

$$[UO_2(OH)_4]^{2-}(aq) + OH^-(aq) \leftrightarrow [UO_2(OH)_5]^{3-}(aq) \quad (1)$$

It appeared as though the equilibrium would be shifted toward the right-hand side of eq 1. Of particular relevance, though, is the highly unusual finding of a facile oxo-ligand exchange between equatorial and axial positions. This process, which has an experimentally observed, rather low activation energy of $\Delta H^{\ddagger} = 9.8 \pm 0.7$ kcal/mol, is highly unusual because it runs counterintuitive to the well-known stability of the uranyl bond (which is thought to be a partial triple bond[56,57]). The work by Clark et al.[45] has prompted a number of further experimental and theoretical studies devoted to the complexation of UO_2^{2+} with hydroxide.[5,14,35,44,48,50,51,53,55]

In 1998, Schreckenbach et al.[44] studied different conformers and transition states of uranyl tetrahydroxide, $[UO_2(OH)_4]^{2-}$, theoretically. They accounted for scalar relativistic effects through large-core effective core potentials (LC-ECP) and employed density functional theory (DFT)[58] with the hybrid functional B3LYP.[59−62] The existence of "*cis*-uranyl" conformers possessing a bent ("*cis*") uranyl bond was predicted. The authors suggested a mechanism for the intramolecular oxygen exchange in a two-step process involving the "*cis*-uranyl" as an intermediate with an activation energy of 38 kcal/mol in the gas phase. They also proposed a mechanism of proton shuttling through water molecules for this phenomenon. Stable "*cis*-uranyl" structures were also predicted for the tetrafluoro and tetrachloro complexes of uranyl(VI) in a subsequent study.[5] We note in passing that an experimental realization of any kind of observable "*cis*-uranyl" structures has been elusive until very recently.[63]

Wahlgren et al.[14] studied the complexation of the uranyl cation with hydroxide ions and water molecules. They found mononuclear hydroxide complexes and an equatorial coordination number of 4.5 ± 0.4 from experimental EXAFS studies. Comparing their calculated bond lengths for the equatorial ligands $U-O_{eq}$ to the experimental EXAFS results, they propose that the four-coordinated species is predominant in the highly alkaline aqueous solutions. (In other words, the equilibrium eq 1 would be shifted toward the left-hand side of eq 1.)

Tsushima and Reich[48] carried out a theoretical study of uranyl hydroxide for monomeric and dimeric complexes using DFT (B3LYP). In a study by Yoshihiro et al.[35] in 2002, structures and charge distributions of different uranyl hydrate and/or hydroxide complexes were investigated theoretically. Ingram

(19) Gresham, G. L.; Gianotto, A. K.; Harrington, P. D.; Cao, L. B.; Scott, J. R.; Olson, J. E.; Appelhans, A. D.; Van Stipdonk, M. J.; Groenewold, G. S. *J. Phys. Chem. A* **2003**, *107*, 8530.
(20) Gianguzza, A.; Milea, D.; Millero, F. J.; Sammartano, S. *Mar. Chem.* **2004**, *85*, 103.
(21) Neuefeind, J.; Soderholm, L.; Skanthakumar, S. *J. Phys. Chem. A* **2004**, *108*, 2733.
(22) Vallet, V.; Szabó, Z.; Grenthe, I. *J. Chem. Soc., Dalton Trans.* **2004**, 3799.
(23) Gibson, J. K.; Haire, R. G.; Santos, M.; Marçalo, J.; de Matos, A. P. *J. Phys. Chem. A* **2005**, *109*, 2768.
(24) Spencer, S.; Gagliardi, L.; Handy, N. C.; Ioannou, A. G.; Skylaris, C.-K.; Willets, A.; Simper, A. M. *J. Phys. Chem. A* **1999**, *103*, 1831.
(25) Blaudeau, J. P.; Zygmunt, S. A.; Curtiss, L. A.; Reed, D. T.; Bursten, B. E. *Chem. Phys. Lett.* **1999**, *310*, 347.
(26) Hay, P. J.; Martin, R. L.; Schreckenbach, G. *J. Phys. Chem. A* **2000**, *104*, 6259.
(27) Hemmingsen, L.; Amara, P.; Ansoborlo, E.; Field, M. J. *J. Phys. Chem. A* **2000**, *104*, 4095.
(28) Matsika, S.; Pitzer, R. M.; Reed, D. T. *J. Phys. Chem. A* **2000**, *104*, 11983.
(29) Tsushima, S.; Suzuki, A. *J. Mol. Struct. (THEOCHEM)* **2000**, *529*, 21.
(30) Tsushima, S.; Yang, T. X.; Suzuki, A. *Chem. Phys. Lett.* **2001**, *334*, 365.
(31) Vallet, V.; Wahlgren, U.; Schimmelpfennig, B.; Szabó, Z.; Grenthe, I. *J. Am. Chem. Soc.* **2001**, *123*, 11999.
(32) Yang, T. X.; Tsushima, S.; Suzuki, A. *J. Phys. Chem. A* **2001**, *105*, 10439.
(33) Fuchs, M. S. K.; Shor, A. M.; Rösch, N. *Int. J. Quantum Chem.* **2002**, *86*, 487.
(34) Greathouse, J. A.; O'Brien, R. J.; Bemis, G.; Pabalan, R. T. *J. Phys. Chem. B* **2002**, *106*, 1646.
(35) Oda, Y.; Aoshima, A. *J. Nucl. Sci. Technol.* **2002**, *39*, 647.
(36) Bridgeman, A. J.; Cavigliasso, G. *Faraday Discuss.* **2003**, *124*, 239.
(37) Clavaguera-Sarrio, C.; Brenner, V.; Hoyau, S.; Marsden, C. J.; Millie, P.; Dognon, J. P. *J. Phys. Chem. B* **2003**, *107*, 3051.
(38) Moskaleva, L. V.; Krüger, S.; Spörl, A.; Rösch, N. *Inorg. Chem.* **2004**, *43*, 4080.
(39) Vallet, V.; Privalov, T.; Wahlgren, U.; Grenthe, I. *J. Am. Chem. Soc.* **2004**, *126*, 7766.
(40) (a) Shamov, G. A.; Schreckenbach, G. *J. Phys. Chem. A* **2005**, *109*, 10961. (b) Correction note: Shamov, G. A.; Schreckenbach, G. *J. Phys. Chem. A* **2006**, *110*, 12072.
(41) Gutowski, K. E.; Dixon, D. A. *J. Phys. Chem. A* **2006**, *110*, 8840.
(42) Bühl, M.; Kabrede, H.; Diss, R.; Wipff, G. *J. Am. Chem. Soc.* **2006**, *128*, 6357.
(43) Szabo, Z.; Toraishi, T.; Vallet, V.; Grenthe, I. *Coord. Chem. Rev.* **2006**, *250*, 784.
(44) Schreckenbach, G.; Hay, P. J.; Martin, R. L. *Inorg. Chem.* **1998**, *37*, 4442.
(45) Clark, D. L.; Conradson, S. D.; Donohoe, R. J.; Keogh, D. W.; Morris, D. E.; Palmer, P. D.; Rogers, R. D.; Tait, C. D. *Inorg. Chem.* **1999**, *38*, 1456.
(46) Moll, H.; Reich, T.; Szabo, Z. *Radiochim. Acta* **2000**, *88*, 411.
(47) Vallet, V.; Wahlgren, U.; Schimmelpfennig, B.; Moll, H.; Szabo, Z.; Grenthe, I. *Inorg. Chem.* **2001**, *40*, 3516.
(48) Tsushima, S.; Reich, T. *Chem. Phys. Lett.* **2001**, *347*, 127.
(49) Sonnenberg, J. L.; Hay, P. J.; Martin, R. L.; Bursten, B. E. *Inorg. Chem.* **2005**, *44*, 2255.
(50) Hratchian, H. P.; Sonnenberg, J. L.; Hay, P. J.; Martin, R. L.; Bursten, B. E.; Schlegel, H. B. *J. Phys. Chem. A* **2005**, *109*, 8579.
(51) Infante, I.; van Stralen, B.; Visscher, L. *J. Comput. Chem.* **2006**, *27*, 1156.
(52) Garcia-Hernandez, M.; Willnauer, C.; Krüger, S.; Moskaleva, L. V.; Rösch, N. *Inorg. Chem.* **2006**, *45*, 1356.
(53) Ingram, K. I. M.; Häller, L. J. L.; Kaltsoyannis, N. *Dalton Trans.* **2006**, 2403.
(54) Siboulet, B.; Marsden, C. J.; Vitorge, P. *Chem. Phys.* **2006**, *326*, 289.
(55) Szabo, Z.; Grenthe, I. *Inorg. Chem.* **2007**, *46*, 9372.
(56) Denning, R. G. *Struct. Bonding (Berlin)* **1992**, *79*, 215.
(57) Denning, R. G. *J. Phys. Chem. A* **2007**, *111*, 4125.
(58) Koch, W.; Holthausen, M. C. *A Chemist's Guide to Density Functional Theory*; Wiley Verlag Chemie: New York, 2000.
(59) Becke, A. D. *Phys. Rev. A* **1988**, *38*, 3098.
(60) Becke, A. D. *J. Chem. Phys.* **1993**, *98*, 5648.
(61) Lee, C.; Yang, W.; Parr, R. G. *Phys. Rev. B: Condens. Matter* **1988**, *37*, 785.
(62) Stephens, P. J.; Devlin, F. J.; Chabalowski, C. F.; Frisch, M. J. *J. Phys. Chem.* **1994**, *98*, 11623.
(63) Vaughn, A. E.; Barnes, C. L.; Duval, P. B. *Angew. Chem., Int. Ed.* **2007**, *46*, 6622.

et al.[53] studied possible geometric and electronic structures for uranyl hydrate and/or hydroxide with the total coordination number of five. They included solvation effects into their DFT calculations using the ADF and G03 packages. The authors concluded that, in highly alkaline solutions, uranyl tetrahydroxide is more favorable energetically than the pentahydroxide (cf. Eq. 1). A combined quantum-mechanics/ molecular mechanics (QM/MM) study was performed on the aqueous solvation of the uranyl hydroxide ion by Infante et al.[51]

Hratchian et al.[50] revisited the axial−equatorial oxo-ligand exchange by modifying the two-step mechanism originally proposed by Schreckenbach et al.[44] They used the more accurate small-core ECPs (SC-ECP) and studied the $[UO_2(OH)_2]$ species in the gas phase as a model system. By including one explicit water molecule to facilitate proton shuttle, they obtain an activation energy of about 23 kcal/mol. We note that this calculated activation energy is still far higher than the experimentally observed one, and we conclude that the question of the detailed ligand exchange mechanism has not been solved thus far.

Very recently, Szabo and Grenthe published an experimental study[55] of the reactivity of the axial oxygen in a number of uranyl(VI) complexes. Whereas the focus is on low pH solutions, where they propose a mechanism involving a bimetallic intermediate, they have also revisited the experiments of Clark et al.[45] on $[UO_2(OH)_{4/5}]^{2-/3-}$ in highly alkaline solutions. They propose that the dynamic processes observed would pertain to the $[UO_2(OH)_4]^{2-}/[UO_2(OH)_5]^{3-}$ equilibrium Eq. (1), and would not, in fact, be an oxygen exchange at all.

The goal of the current study is to solve the 12-year-old "riddle" of the actual mechanism for the facile axial−equatorial oxygen exchange of the uranyl(VI) cation UO_2^{2+} within highly alkaline solutions observed by Clark et al.,[45] assuming that this process is indeed occurring. Besides, the equally controversial question of the equatorial coordination number (equilibrium between tetra- and penta-coordination, Eq. 1) is addressed also.

For the axial−equatorial oxygen exchange, we propose a novel three-step mechanism that involves the following reactions. These reactions are represented schematically in Scheme 1. As a first step, an equilibrium exists between $[UO_2(OH)_4]^{2-}$ and $[UO_2(OH)_5]^{3-}$, eq 1. The next step involves water elimination to yield the newly proposed complex $[UO_3(OH)_3]^{3-}$:

$$[UO_2(OH)_5]^{3-}(aq) \rightarrow [UO_3(OH)_3]^{3-}(aq) + H_2O(aq) \quad (2)$$

In a third step, the $[UO_3(OH)_3]^{3-}$ intermediate facilitates the actual oxo-ligand exchange by way of intramolecular proton shuttling, either directly (reaction 3a) or through a water molecule (reaction 3b), Scheme 1:

$$[O=U=O^*(O)(OH)_3]^{3-}(aq) \leftrightarrow [UO_2(O)(O^*H)(OH)_2]^{3-}(aq) \quad (3)$$

In addition, we have also explored the previously suggested *cis*-uranyl mechanism, reaction 4, Scheme 1. These reactions are probed using DFT, two different relativistic methods, and continuum solvation models.

Computational Methods

Two quantum-chemical programs were used for the calculations, the Priroda[64−68] and Amsterdam Density Functional[69−71] (ADF) codes. Gas-phase geometry optimization and energy and frequency calculations were performed with the Priroda code.[64−68]

In the Priroda code, relativistic effects are implemented applying a scalar four-component relativistic method[65,67,68,72] and all the spin−orbit coupling terms are separated from scalar terms and neglected. Because the oxidation state of uranium is (VI) and does not change in the reactions studied, the mentioned approximation and neglect does not create a problem in our calculations. We used all-electron Gaussian basis sets of triple-ζ-plus-polarization (TZP) quality in all our Priroda calculations.[67] (This is the large-component basis set. The basis sets for the small component are more extensive since they were derived by applying a kinetic balance criteria.)

Shamov et al.[40,73,74] have extensively tested the reliability and performance of Priroda as applied to actinide molecules. They carried out Priroda calculations on small molecules such as UO_2^{2+}, UO_2F_2, UOF_4, UO_3, $[UO_2(H_2O)_5]^{2+}$, or UF_6, among others. They found that the results were very similar to the results from other codes, provided the same XC functional and comparable basis sets were applied.

Restricted scalar DFT was applied for all calculations. We used two versions of approximate DFT, the generalized gradient approximation (GGA) functional PBE,[75] and the hybrid functional B3LYP.[59−62] Single-point energy calculations using the B3LYP functional were carried out on the optimized geometries from PBE to compare the energies from optimized and single points in B3LYP calculations.

Optimized geometries of transition states were verified to possess an imaginary harmonic vibrational frequency, which appears as a translational mode in the reaction path coordinate. Harmonic vibrational frequencies were also used in thermochemistry calculations.

Intrinsic reaction coordinates (IRC) calculations in the gas phase were carried out for reactions 1−4 applying Priroda and the PBE functional. By construction, IRC plots are based on the electronic energy (the total, or internal, energy). Priroda uses geometry optimizations in small intervals to construct the minimum energy trajectory on the energy surface. IRC calculations can be used not only for dynamical and kinetic purposes, they can also be applied for the verification of the reactants and products for a given transition state. A total of 100, 120, 188, 55, and 138 geometry optimizations in the reaction paths were carried out for reactions 1, 2, 3a (proton shuttling via the Hydrogen atom), 3b (proton shuttling via the water molecule), and 4, respectively.

Population-based (Mayer)[76] bond orders were calculated with the Priroda−PBE approach. Atomic charges and bond orders are, of course, not quantum-mechanical observables. However, we have found that the calculated charges and bond orders consistently

(64) Laikov, D. N. Priroda code, version 5.0, 2004.
(65) Laikov, D. N. *Chem. Phys. Lett.* **1997**, *281*, 151.
(66) Laikov, D. N. An implementation of the scalar relativistic density functional theory for molecular calculations with Gaussian basis sets. Poster presentation at DFT2000 Conference, Menton, France, June 11–14, 2000.
(67) Laikov, D. N. *Chem. Phys. Lett.* **2005**, *416*, 116.
(68) Laikov, D. N.; Ustynyuk, Y. A. *Russ. Chem. Bull.* **2005**, *54*, 820.
(69) Baerends, E. J.; et al. ADF 2004.01, Scientific Computing and Modelling, Theoretical Chemistry, Vrije Universiteit: Amsterdam, The Netherlands, 2004.
(70) Fonseca Guerra, C.; Snijders, J. G.; te Velde, G.; Baerends, E. J. *Theor. Chem. Acc.* **1998**, *99*, 391.
(71) te Velde, G.; Bickelhaupt, F. M.; Baerends, E. J.; Fonseca Guerra, C.; van Gisbergen, S. J. A.; Snijders, J. G.; Ziegler, T. *J. Comput. Chem.* **2001**, *22*, 931.
(72) Dyall, K. G. *J. Chem. Phys.* **1994**, *100*, 2118.
(73) Shamov, G. A.; Schreckenbach, G. *J. Phys. Chem. A* **2006**, *110*, 9486.
(74) Shamov, G. A.; Schreckenbach, G.; Vo, T. *Chem. Eur. J.* **2007**, *13*, 4932.
(75) Perdew, J. P.; Burke, K.; Ernzerhof, M. *Phys. Rev. Lett.* **1996**, *77*, 3865.
(76) Mayer, I. *Simple theorems, proofs, and derivations in quantum chemistry*; Kluwer Academic/Plenum Publishers: New York, 2003.

Scheme 1. Schematic Representation of Reactions 1 to 4

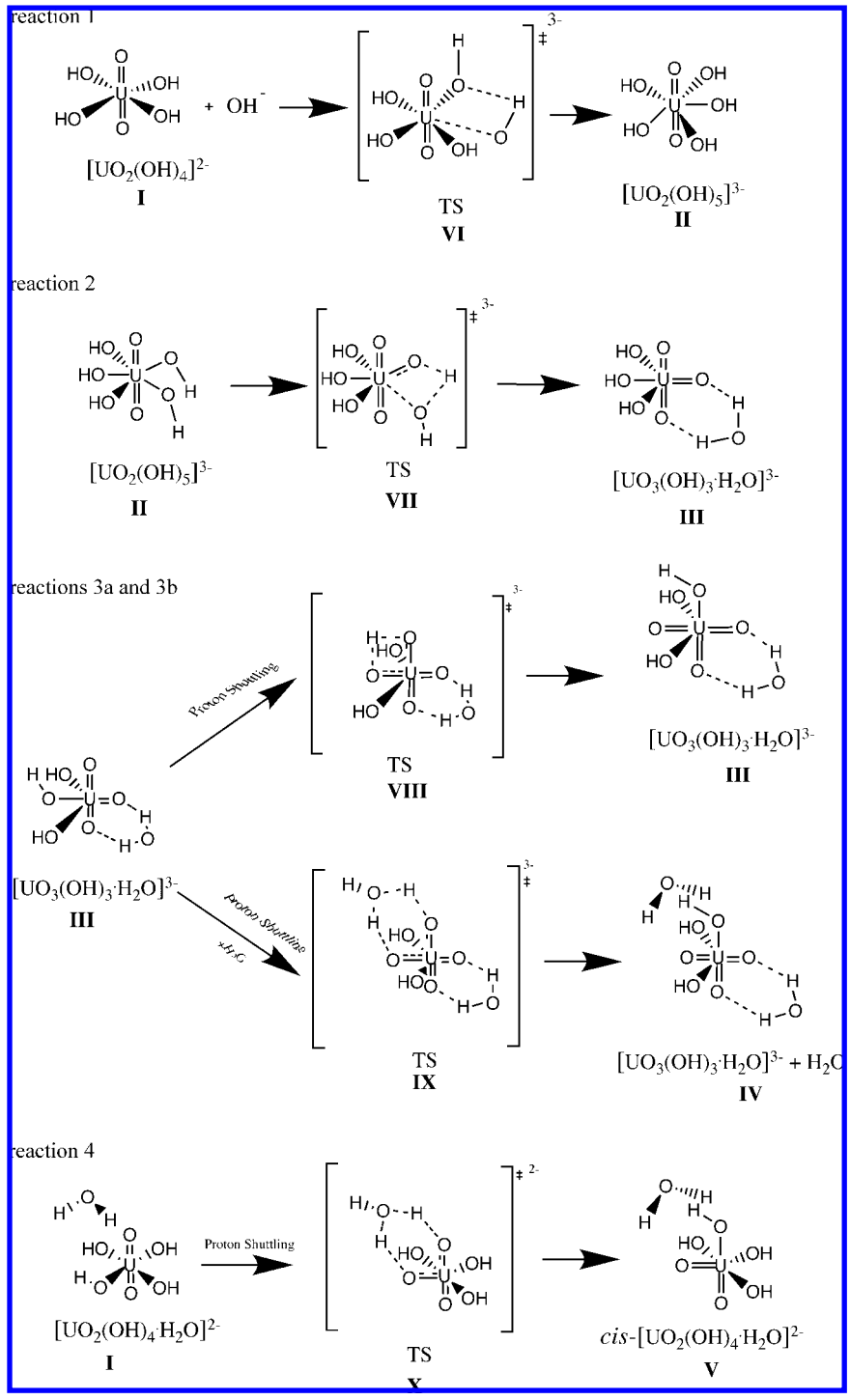

conform to chemically meaningful models for various actinide compounds and various strengths of bonds.[40,73,74,77−79]

The quantum-mechanical modeling of solvation effects is an area of ongoing research.[80] In this work, solvation effects on geometries and energies were studied by using the ADF code,[69−71] which applies the COSMO solvation model for this purpose.[81−83]

In the ADF code, relativistic effects were modeled through the zeroth order regular approximation (ZORA) method.[84−87] We used

(77) Shamov, G. A.; Schreckenbach, G. *Inorg. Chem.* **2008**, *47*, 805.
(78) Berard, J. J.; Shamov, G. A.; Schreckenbach, G. *J. Phys. Chem. A* **2007**, *101*, 10789.
(79) Shamov, G. A.; Schreckenbach, G.; Martin, R. L.; Hay, P. J. *Inorg. Chem.* **2008**, *47*, 1465.
(80) Cramer, C. J.; Truhlar, D. G. *Chem. Rev.* **1999**, *99*, 2161.
(81) Klamt, A.; Jonas, V.; Bürger, T.; Lohrenz, J. C. W. *J. Phys. Chem. A* **1998**, *102*, 5074.
(82) Klamt, A.; Schüürmann, G. *J. Chem. Soc., Perkin Trans.* **1993**, *2*, 799.
(83) Pye, C. C.; Ziegler, T. *Theor. Chem. Acc.* **1999**, *101*, 396.
(84) van Lenthe, E.; Baerends, E. J.; Snijders, J. G. *J. Chem. Phys.* **1993**, *99*, 4597.

triple-ζ-plus-polarization (TZP) basis sets in the ADF calculations. ADF applies Slater type orbitals (STO) and numerical integration in the SCF procedure. We chose a numerical integration parameter of 5.5 in this type of calculations.

In most of the ADF-COSMO calculations, a solvent-excluding surface and the Klamt[81] radii for hydrogen and oxygen were used. These radii are $R_H = 1.30$ Å and $R_O = 1.72$ Å, respectively. For the uranium atom, a radius of $R_U = 1.70$ Å was applied. COSMO geometry optimizations were carried out for the species in the bottleneck reactions, reactions 1 and 3, in order to get a better estimate of the possible activation energies, which can be influenced by the surroundings.

In order to check the stability of the calculations against the parameters of the solvation model, notably the radii and cavity model, we have also determined the reaction energies (ΔH and ΔG) for one of the reactions, reaction 3b (see also below) using the COSMO parameters of Ingram et al.[53] These parameters are $R_H = 1.20$ Å, $R_O = 1.40$ Å, $R_U = 2.00$ Å, as well as a solvent-accessible surface. The results are collected in Table S1 of the Supporting Information. Although these parameters are significantly different from the ones used elsewhere in this article, there influence on the energetics is essentially negligible, with changes of at most 0.3 kcal/mol in the energies. We conclude that, at least for the systems under study, the reaction energetics (and hence the conclusions that are based on them) are stable against variations in the parameters of the continuum solvation model.

The influence of a second coordination sphere on properties of actinide complexes has been studied by us[40] and others;[41,51,54] see also the recent paper by Jaque et al.[88] Although the second coordination sphere has a certain influence on the results (through direct solvation effects such as charge transfer and hydrogen bond networks), we have concluded that continuum solvation models such as COSMO can cover the bulk of such effects, too, provided the first coordination sphere of directly coordinated solvent molecules is included into the quantum-chemical model.[40] Moreover, issues related to the second coordination sphere (such as number of water molecules, surface effects, conformational space, etc.) would render these kinds of models impractical for the given studies that aim at elucidating a rather complicated reaction mechanism. Finally, it is reasonable to assume that the effects of the second coordination sphere would cancel at least partly between the left- and right-hand sides of any given reaction and/or are included in an average way into the parametrization of the continuum solvation models.[80]

Results and Discussion

This section is organized as follows. We start by discussing, in general terms, various reactions that are part of possible pathways for the intramolecular oxygen exchange in uranyl hydroxide. Next, we discuss the geometries and vibrational frequencies of key species, followed by reaction energies. We conclude with some general discussions.

Reactions and Intrinsic Reaction Coordinates. A total of five reactions were studied. The first four reactions, reactions 1, 2, 3a, and 3b, were studied in order to examine our proposed mechanism and the fifth reaction, reaction 4, to compare our results for the four-OH coordinated uranyl to the previous results for uranyl hydroxides. Schematic representations of reactions 1−4 are shown in Scheme 1.

As discussed in the introduction, the mechanism which was suggested by Schreckenbach et al.[44] and further investigated by Hratchian et al.[50] for the oxygen exchange in uranyl hydroxide could not satisfy the experimental results energetically. For the sake of completeness, however, we have investigated it, too. (Reaction 4 in Scheme 1 illustrates the principle of that mechanism.) We studied uranyl coordinated with two to five hydroxide ligands. The reaction involving the tetrahydroxide as the starting point is shown in Scheme 1. It is possible to devise a reaction similar to reactions 3a, 3b for uranyl coordinated with two or three OH^- ligands. We have tested this, but the reactions have higher activation energies than those presented here. We will not discuss them any further accordingly.

We got about 15 kcal/mol for the barrier height of proton shuttling through a water molecule in $[UO_2(OH)_4]^{2-}$ in the gas phase (reaction 4), while Hratchian et al.[50] calculated it to be more than 20 kcal/mol. This difference (as compared to experiment) was also observed between the results from ref 44 which considered proton shuttling through a hydrogen atom in the four-coordinated uranyl hydroxide, and the results for the corresponding phenomenon in the two-coordinated uranyl hydroxide in ref 50. We propose that the problem arises because that mechanism contains an intermediate with a bent uranyl structure ("*cis*-uranyl" **V**, the product of reaction 4). Thus, an energetic penalty arises from abandoning the stabilization that is inherent to the linear uranyl unit.

We can avoid these energetically unfavorable *cis*-uranyl structures by suggesting a new configuration for the intermediate species, which, through hydrogen shuttling, can explain the oxygen exchange phenomenon (see Scheme 1, reactions 1−3). The proposed intermediate structure **III** has a T-shaped configuration with a uranium central atom and three double-bonded oxygens attached to it (cf. the reactant and product of reactions 3). Proton shuttling (pseudorotation) in this species preserves a stable, linear uranyl throughout.

In order to get to our suggested intermediate structure from uranyl hydroxide, at first we examined different possible ways and failed to get optimized geometries or reasonable energies. We finally came to the conclusion that it is possible to get the T-shaped configuration through an intramolecular water molecule elimination, reaction 2 (Scheme 1). Considering four-coordinated uranyl hydroxide instead of five-coordinated would leave us with the structure, $[UO_3(OH)_2]^{2-}$. This species is coordinatively unsaturated and is therefore not a favorable intermediate (in terms of relative energies) in order to get the linear O═U═O structure in the oxygen-exchanged uranyl hydroxide. Furthermore, the strong equatorial U−OH bonds in $[UO_2(OH)_4]^{2-}$ would not allow a proton detachment in order to eliminate a water molecule and get the $[UO_3(OH)_2]^{2-}$ structure. However, if we start with the five-coordinated uranyl hydroxide, not only is our first desire for water elimination satisfied but also it will result in a symmetric structure which will contribute to the essential step reactions 3a or 3b with much less activation energy.

The first two reactions in Scheme 1 bring us to the mentioned T-shaped uranyl intermediate **III**. The third and fourth reactions (reactions 3a and 3b) are the two possible pathways for transferring a hydrogen atom from an equatorial OH^- to the axial oxygen. One might consider either all of the first three reactions (1−3a or 1−3b) as two possibilities for a multistep mechanism, which occur consequently until we get to exchanged-oxygen uranyl hydroxide, or the reactions 3a or 3b as the essential mechanism.

(85) van Lenthe, E.; Baerends, E. J.; Snijders, J. G. *J. Chem. Phys.* **1994**, *101*, 9783.
(86) van Lenthe, E.; Ehlers, A.; Baerends, E. J. *J. Chem. Phys.* **1999**, *110*, 8943.
(87) van Lenthe, E.; van Leeuwen, R.; Baerends, E. J. *Int. J. Quantum Chem.* **1996**, *57*, 281.
(88) Jaque, P.; Marenich, A. V.; Cramer, C. J.; Truhlar, D. G. *J. Phys. Chem. C* **2007**, *111*, 5783.

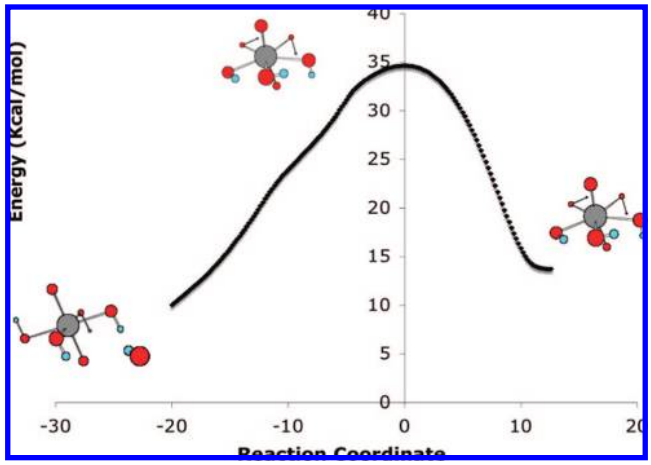

Figure 1. Intrinsic reaction coordinate for reaction 1 and PBE-optimized structures for the reactant **I**, transition state **VI**, and product **II**.

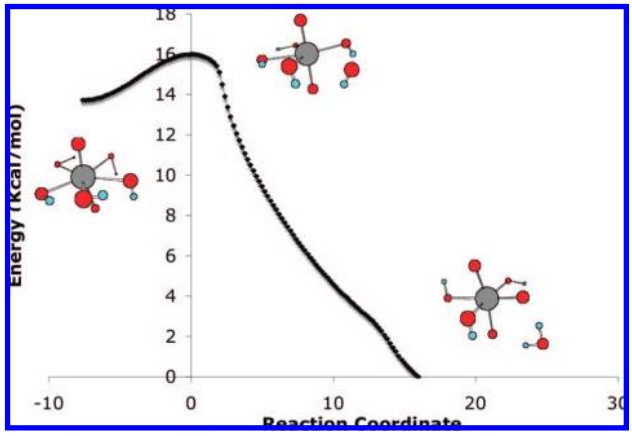

Figure 2. Intrinsic reaction coordinate for reaction 2 and PBE-optimized structures for the reactant **II**, transition state **VII**, and product **III**.

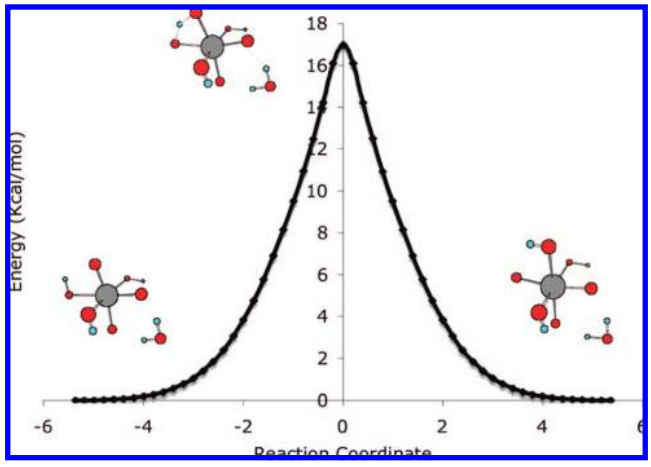

Figure 3. Intrinsic reaction coordinate for reaction 3a and PBE-optimized structures for the reactant **III**, transition state **VII**, and product **III**.

Using intrinsic reaction coordinate (IRC) calculations we obtained the reaction path for each step of the mechanism. IRC plots for these reactions are shown in Figures 1−4. We have also included the optimized structures of the respective reactants, transition states and products. Figure 5 shows the IRC plot for the alternative reaction mechanism, reaction 4. Finally, in Figure 6, we present combined IRC plots for the "proton shuttling via hydrogen" mechanism (reactions 1, 2, 3a, Figure 6a) and the

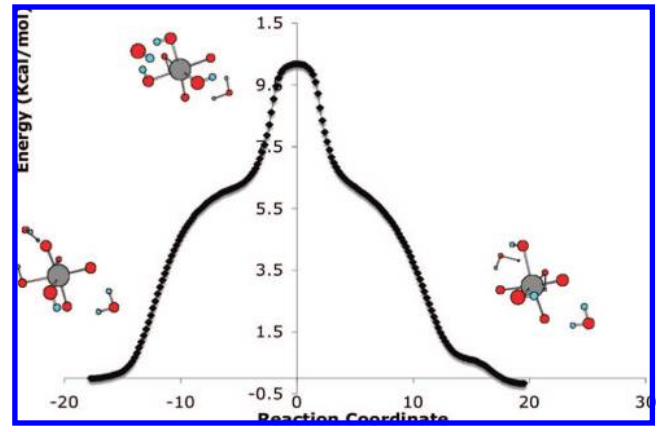

Figure 4. Intrinsic reaction coordinate for reaction 3b and PBE-optimized structures for the reactant **III**·H_2O, transition state **IX**, and product **III**·H_2O.

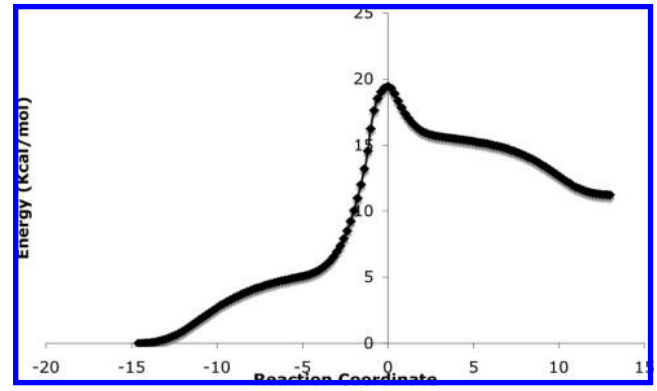

Figure 5. Intrinsic reaction coordinate for reaction 4.

"proton shuttling via water" mechanism (reactions 1, 2, 3b, Figure 6b), respectively.

It is instructive to consider the shapes of the different IRC plots in some detail. For reactions 3a and 3b, we have symmetrical reaction coordinates because of the similarity between reactants and products. The reaction coordinate for the reaction 3a has a regular peak shape, which means only changes in two O−H bonds along the reaction coordinate are involved in shaping it. However, the case is different in reaction 3b where the shuttling happens through a water molecule. Here, not only are the two OH bonds along the reaction coordinate responsible for the overall shape but the third OH also makes some changes resulting in deviations from an exact peak-shaped curve. Similar factors make the IRC figure for reaction 4 deviate from a regular endothermic reaction coordinate.

IRC curves could, in principle, be used for an analysis of the kinetics and dynamics of the reactions, and information such as tunneling parameters could be obtained (see also below). However, this is beyond the scope of the current investigations.

Geometries, Vibrational Frequencies, and Bond Orders. Calculated optimized geometries of all species in the gas phase are tabulated in Table 1. Symmetric and antisymmetric uranyl stretching frequencies for the different UO_2^{2+} and UO_3 species and imaginary frequencies for transition states are also given in that table. There is a good inverse correlation between bond lengths and stretching frequencies; with the increase in bond lengths there is a decrease in stretching vibration frequencies. We note, in particular, the decrease in both symmetric and antisymmetric stretching frequencies in going from [UO_2-

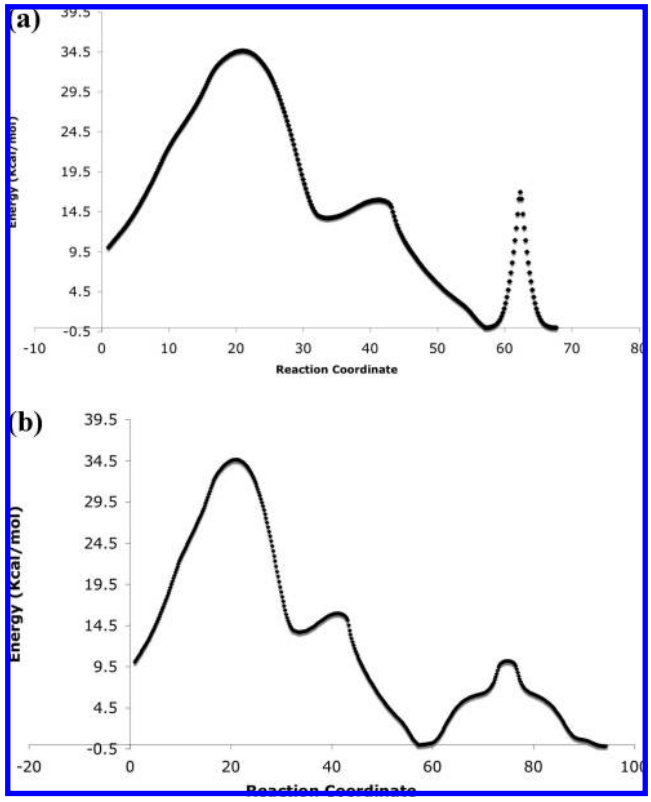

Figure 6. Combined intrinsic reaction coordinate plots for the proposed mechanism: (a) "proton shuttling via hydrogen" mechanism, reactions 1, 2, 3a; (b) "proton shuttling via water" mechanism, reactions 1, 2, 3b.

$(OH)_4]^{2-}$ **I** to $[UO_2(OH)_5]^{3-}$ **II**, Table 1. Comparing the two structures of four- and five-coordinated uranyl hydroxides, there is a significant difference (about 11°) between O═U═O angles with the uranyl unit of **I** being essentially linear and that of **II** being slightly bent.

There is also an increase in equatorial U−O(H) (hydroxide) bond lengths, especially for the fifth hydroxide ligand that indicates its instability. This unstable U−O(H) bond contributes to our proposed water elimination mechanism, reaction 2. However, even the longest of the U−O(H) bonds at 2.479 Å is short enough for the ligand to be in the first coordination sphere of the metal.

In Table 1 we have also included the calculated bond lengths and angles in solution for some of the species. In going from gas phase to the condensed phase, there is an increase in O═U═O angle and a decrease in axial U−O bonds in the five-coordinated uranyl hydroxide and its descendents in the next reactions, Table 1. Equatorial bond lengths are, in general, longer in solution than the gas phase, which can be readily understood by the solvent stabilization of the negatively charged OH^- ligands. Overall, the solution structures are less tight and more stable than the gas phase structures. This can be contrasted to the case of the uranyl penta-aquo complexes $[UO_2(H_2O)_5]^{1+/2+}$ that possesses neutral equatorial ligands.[40] For these systems, we observe a marked decrease of the equatorial bond lengths upon solvation, both using microsolvation (up to 12 additional water molecules in the second coordination sphere) and continuum solvation similar to the model employed in the current study.

In Table 2, we provide a comparison between our calculated axial and equatorial U−O bonds and U═O stretching frequencies and those of previous experimental or theoretical studies for tetra- and pentauranyl hydroxides.[14,44−49,53]

Because previous experimental or calculated data are only available for four- and five-coordinated uranyl hydroxide we provide only bond lengths and frequencies of these species in comparison to the available data. Experimental data exists for the four-coordinated uranyl hydroxide only. For the five-coordinated species, there is only previous calculated data available (though, as discussed in the introduction, it is not entirely clear which coordination number actually predominates in solution.) Comparing the PBE gas phase numbers, we find good agreement between our calculated U−O bond lengths and the previous calculated bond lengths for both the four- and five-coordinated uranyl hydroxide. Both, the axial and equatorial bond lengths of $[UO_2(OH)_4]^{2-}$ are overestimated by our gas phase calculations if compared to the experimental data[45,46] or the B3LYP results by about 0.06 Å, Table 2. This corresponds to the tendency of GGA functionals to overestimate bond lengths that has been observed for various actinide species.[40,73,74,79]

Table 1. Calculated Angles, Bond Lengths, Uranyl Stretching Frequencies of Different Species, and Imaginary Frequencies for Transition States in the Gas Phase (Priroda TZP-PBE) and Solution (ADF COSMO TZP-PBE) (bond lengths, Å; bond angles, deg; frequencies, cm^{-1})[a]

	U═O	O═U═O angle	U−OH	U−O−H	ν_{sym}[b]	ν_{asym}[b]	ν_i[c]	b-bond[d]	f-bond[d]
I (gas)	1.873	179.7	2.285−2.290	99.9−100.5	728	800			
I (soln)									
II (gas)	1.879, 1.903	168.8	2.311−2.479	82.9−89.2	704	778			
II (soln)	1.887, 1.886	172.9	2.342−2.444	89.1−106.5					
III (gas)	1.933, 1.953, 2.01	169.1, 98.1, 90.7	2.389−2.394	88.4−92.0	684	531, 644			
III (soln)	1.922, 1.933, 2.033	172.8, 93.7, 92.3	2.303−2.360	104.8, 106.6					
IV (gas)	1.946, 2.010	172.9, 90.9	2.295−2.477	90.8−98.2	685	543, 648			
IV (soln)	1.922, 1.935, 2.028	174.6, 92.4, 93.1	2.289−2.401	105.1−109.1					
V (gas)	1.920, 1.944	98.3	2.168−2.364	100.0−105.1	736	630			
V (soln)	1.904, 1.937	96.2	2.219−2.261	107.2−113.9					
VI (gas)	1.868, 1.887	170.8	2.308−2.386	89.0−93.6	720	786	113i		3.776
VI (soln)	1.876, 1.878	175.7	2.263−2.329	99.0, 107.4					3.733
VII (gas)	1.884, 1.904	170.6	2.213−2.423	85.0−92.9	675	761	101i	2.980	1.533
VIII (gas)	1.987, 2.115	166.8, 99.6, 92.4	2.115, 2.372	72.5, 91.0	678	633, 518	1410i	1.256	1.256
IX (gas)	1.971, 1.972, 2.141	172.8, 94.0, 91.6	2.136−2.348	93.0, 109.2	672	574	96i	1.058, 1.586	1.054, 1.575
X (gas)	1.907, 2.068	176.8	2.061−2.270	101.4−111.3	661	743	515i	1.160, 1.521	1.066, 1.319

[a] **I** = $[UO_2(OH)_4]^{-2}$, **II** = $[UO_2(OH)_5]^{-3}$, **III** = $[UO_3(OH)_3 \cdot H_2O]^{-3}$, **IV** = $[UO_3(OH)_3 \cdot H_2O \cdot H{-}O{-}H]^{-3}$, **V** = *cis*-$[UO_2(OH)_4 \cdot H{-}O{-}H]^{-2}$, **VI** = $[UO_2(OH)_4{-}OH]^{-3\#}$, **VII** = $[UO_3(OH)_3 \cdot H{-}OH]^{-3\#}$, **VIII** = $[UO_3(OH)_3 \cdot H_2O]^{-3\#}$ (H shuttling), **IX** = $[UO_3(OH)_3 \cdot H_2O\ HOH]^{-3\#}$ (H shuttling), **X** = $[UO_2(OH)_4 \cdot HOH]^{-2\#}$ (H shuttling). The structures on the different species are shown in Scheme 1. [b] ν_{sym} = Symmetric stretching frequency for O═U═O; ν_{asym} = Antisymmetric stretching frequency for O═U═O. [c] ν_i = Imaginary frequency for the transition states. [d] For transition states, "b-bond" and "f-bond" refer to the bond broken and bond formed, respectively.

Table 2. Calculated *r*(U═O) (Å), *r*(U−O(H) (Å), and Symmetric and Antisymmetric O═U═O Frequencies (cm^{-1}) and Some Previous Experimental and Theoretical Data for the Tetra- and Pentacoordinated Uranyl Hydroxides

	species							
	$[UO_2(OH)_4]^{2-}$				$[UO_2(OH)_5]^{3-}$			
code, functional	U═O	U−O_h	ν_{sym}	ν_{asym}	U═O	U−O_h	ν_{sym}	ν_{asym}
Priroda, PBE	1.873	2.285−2.290	728	800	1.879, 1.903	2.311−2.479	704	778
ADF COSMO, PBE					1.887, 1.886	2.342−2.444		
Experimental Results								
ref 45: EXAFS (solid)	1.810	2.210	796					
ref 45: EXAFS (soln.)[a]	1.790	2.220	786					
ref 45: XRD	1.820	2.260						
ref 46: EXAFS	1.830	2.260						
Previous Theoretical Results								
ref 53: ADF, PBE, gas	1.875	2.309	738	814	1.879	2.465	713	789
ref 53: G03, PBE, gas	1.873	2.283	727	809	1.884	2.415	677	
ref 53: ADF COSMO, PBE	1.873	2.294	726	808	1.881		709	789
ref 14: B3LYP	1.800							
ref 49: B3LYP	1.841	2.309	762	833	1.835	2.462	750	822
ref 47: AIMP gas	1.770	2.336						
ref 47: AIMP CPCM	1.760	2.300						
ref 44: B3LYP	1.842	2.334	739	823				

[a] According to the authors, the solution species is likely the pentahydroxide.

Table 3. Bond Orders in Reactions 2 and 3, Calculated at the Priroda TZP-PBE Level

reaction 2				reaction 3a				reaction 3b		
bond	reactant **II**	TS **VII**	product **III**	bond	reactant **III**	TS **VIII**	product **III**	reactant **III**	TS **IX**	product **IV**
U1−O5	0.94	0.6	0.1	U1−O3	2.06	2.10	2.14	2.16	2.13	2.17
U1−O3	1.15	1.39	2.07	U1−O2	2.14	2.10	2.06	2.08	2.12	2.09
U1−O2	2.27	2.27	2.14	U1−O4	1.08	1.63	2.28	1.13	1.42	2.16
U1−O1	2.28	2.28	2.28	U1−O1	2.28	1.63	1.08	2.16	1.41	1.13

(Note that hybrid functionals such as B3LYP tend to underestimate bond lengths, though.)

Since the proposal of a $[UO_3(OH)_3]^{3-}$ intermediate is a central result of this study, it is worthwhile to look at its properties separately, too. Specifically, we have studied species **III**, the molecule microsolvated with one water molecule as it appears in the proposed mechanism reaction 3b. From Table 1, we see that the UO_3 core of the molecule has an approximate T-shaped geometry with two short U═O bonds and one longer one, corresponding to a linear uranyl with an equatorial oxo ligand (or, in other words, a uranyl oxide.) Previously, we have found the naked UO_3 molecule to have a similar type of conformation.[74] The calculated vibrational frequencies for molecule **III** have been collected in Table S2 of the Supporting Information.

Let us now turn to the data in Table 3. A track of axial and equatorial U−O bond orders that are active during reactions 2 and 3 are given in that table. In reaction 2, the U−O5 bond, which is an equatorial U−O bond and has a bond order of 0.94 in the reactant, contributes to the water elimination. Consequently, this bond order is reduced to 0.1 in the product. U−O3 is another equatorial U−O bond. It has a bond order of 1.15 in the reactant indicating a relatively strong single bond (actually partial double bond character, see below.) In reaction 2, this oxygen loses its proton, resulting in a bond order of 2.07, i.e. an equatorial multiple bond. Indeed, we note that the bond order is larger than two, indicating a partial triple bond. The bond orders for the axial bonds, U−O1 and U−O2, remain almost the same in reaction 2. They are partial triple bonds, too, which is generally the case for uranyl complexes. In reactions 3a and 3b, U−O4, another equatorial bond, loses the proton and its bond order changes from 1.08 to 2.28 for reaction 3a and from 1.13 to 2.16 for reaction 3b. The axial bond U−O1 gains that proton through hydrogen shuttling and changes to become a single bond. The bond orders in the transition states for the active bond during the reaction are about an average of the respective bond orders in reactants and products.

Note that most of the U−O(H) bonds have calculated bond orders larger than unity, indicating some amount of π-donation from the OH^- ligand to the metal. This results in the mentioned partial double bond character for this equatorial ligand. Previously, we have pointed out that these relatively strong equatorial bonds that go along with π-competition at the metal center result in a relatively low energy for the *cis*-uranyl conformer, by destabilizing the (trans) ground state.[5,44]

Energies and Reaction Pathways. The barrier height enthalpies and Gibbs free energies for the forward and backward reactions and the overall enthalpies and Gibbs free energies of the reactions in the gas phase are presented in Table 4. In this table, all the energies were corrected to correspond to room temperature, 25 °C, 298 K.

The calculated barrier height for the first step in the gas-phase (considering corrected energies at 25 °C) is $\Delta H^{\ddagger} = 120.7$ kcal/mol. We also calculated the barrier height for this reaction in solution by employing the COSMO model. We found a significant decrease in the barrier height. A barrier height of only $\Delta H^{\ddagger} = 12.5$ kcal/mol was found for this reaction in solution. We think that this significant difference originates primarily from the modeling of a bare OH^- in the COSMO model, given that a polarizable solvent will most strongly stabilize a compact charged, species.

Because the four-coordinated uranyl hydroxide is energetically more stable than the five-coordinated uranyl hydroxide (calculated reaction free energies ΔG of 111.2 and 13.2 kcal/mol for gas phase and solution, respectively), it might seem that this reaction is unlikely to happen. However, in the next step (reaction 2), by a small activation energy of about 1 kcal/

Table 4. Barrier Height Enthalpies and Gibbs Free Energies of the Forward (F) and Backward (B) Reactions for Reactions 1 to 4[a]

	reaction 1		reaction 2		reaction 3a		reaction 3b		reaction 4	
optimization (PBE)	gas	solv	gas	solv	gas	solv	gas	solv	gas	solv
ΔH^{F}	120.7	12.5	1.0		14.5		7.8	5.1	15.5	11.5
ΔH^{B}	19.8	9.5	15.2		14.5		7.9	4.9	4.5	
ΔH_{298}	100.9	3.0	−14.2		0.0		−0.1	0.2	11.0	
ΔG^{F}	129.5	21.3	1.6		15.5		8.4	5.7	15.6	11.6
ΔG^{B}	18.4	8.0	16.6		15.6		8.7	5.7	4.7	
ΔG_{298}	111.2	13.3	−14.9		−0.1		−0.3	0.0	10.8	

	reaction 1		reaction 2		reaction 3a		reaction 3b		reaction 4	
gas-phase (B3LYP)	opt	S.P.	opt	S.P.	opt	S.P.	opt	S.P.	opt	S.P.
ΔH^{F}		100.8		3.7	13.7	13.2	6.8	6.8		
ΔH^{B}		16.9		14.5	13.7	13.2	6.7	6.8		
ΔH_{298}		83.9		−10.8	0.0	0.0	0.1	0.0		
ΔG^{F}		109.7		4.4	15.1	14.2	7.1	7.4		
ΔG^{B}		15.4		15.9	15.1	14.2	6.8	7.6		
ΔG_{298}		94.3		−11.5	0.0	0.0	0.3	−0.2		

[a] ΔH_{298} and ΔG_{298} correspond to the overall reactions (all energies are in kcal/mol) "S.P." and "opt" refer to single-point calculations and full optimizations, respectively (see text).

mol, we could get to a much more stable species in solution, $[UO_3(OH)_3 \cdot H_2O]^{3-}$, which can facilitate the intramolecular oxygen exchange. Moreover, reaction 2 involves elimination of a water molecule. We note that the experimental conditions used by Clark et al.[45] involved high-ionic-strength solutions of Na(OH) (as high as 3 M). Each solvated Na^+ ion binds approximately six water molecules in its first solvation shell. As a consequence, the concentration of free water is significantly reduced as compared to the neat liquid, driving reaction 2 further to the right-hand side. These kinds of collective effects cannot be captured by our relatively simple solvation model.

The hydrogen transfer between axial and equatorial oxygens in $[UO_3(OH)_3 \cdot H_2O]^{3-}$ (reactions 3a and 3b) can occur through a hydrogen atom or a water molecule. The calculated activation energies for these reactions in the gas phase are 14.5 and 7.8 kcal/mol for these reactions, respectively (using the PBE functional). The activation energy for reaction 3b is further reduced to 5.1 kcal/mol in solution.

The absolute values of the different activation energies are crucial for the conclusions of this study, and it is therefore important to test the influence of the different approximations. While we are confident regarding the relativistic approximations, ZORA and all-electron scalar, respectively,[40,73,74] and the basis sets (essentially converged), we have also calculated the activation energies for these reactions using the B3LYP functional. In this way, we can test the choice of model chemistry. Two different approaches have been investigated. One approach encompassed calculating activation energies from B3LYP-optimized geometries. In the other approach, single point B3LYP energy calculations were carried out using the optimized PBE geometries. In both approaches we got very similar activation energies of 13.7 vs 13.2 kcal/mol for reaction 3a, and a constant value of 6.8 kcal/mol for reaction 3b, respectively. This justifies calculating B3LYP energies in the single point approach only for the rest of our species. Comparing the activation energies in PBE and B3LYP, there is a slight difference of 1 kcal/mol or less. This result is very reassuring because it shows that the B3LYP and PBE functionals have a very similar influence on the energies of reactant and transition states for our reactions.

The influence of the parameters of the solvation model has been tested also (see the Computational Details, and Table S1 in Supporting Information), and the results have been found to be stable in this respect, too.

Discussion

As outlined above, we have proposed a new mechanism for the experimentally observed facile oxo-ligand exchange in uranyl hydroxide between the axial and equatorial positions. The key feature of our proposal is the $[UO_3(OH)_3]^{3-}$ intermediate **III**. On the basis of the calculated bond orders (Table 3) and the analogy to the known UO_3 molecule, one could view **III** as a "mixed uranyl oxo hydroxo" complex. As opposed to previous mechanistic proposals involving "*cis*-uranyl" structures such as **V**, reaction 4, **III** avoids the energetic penalty of breaking the extraordinarily stable linear uranyl bond.

The overall bottleneck reaction for our suggested mechanism is the reaction 1. We obtained an activation energy in solution of $\Delta H^{\ddagger} = 12.5$ kcal/mol for this reaction, which is a reasonable activation energy comparing to Clark's experimental result of 9.8 kcal/mol.[45] The remaining difference is of the same order as any uncertainties in the relatively simple solvation model used. We should note, though, that selected tests show that the results are stable against variations in the parameters of the solvation model. Moreover, the choice of the particular DFT method (GGA and hybrid functionals) has only a minor influence on the calculated results. Likewise, the relatively large basis sets used can be considered as essentially converged. These results give confidence again in the calculated numbers, and one can contrast this to cases such as, for instance, the first bond dissociation energy of UF_6 where the influence of the DFT XC functional is considerable.[74,89] Generally, conformational energies are easier to obtain accurately than those for processes involving bond breaking.

The proposed mechanism contains, as a crucial intermediate, the newly proposed trioxide species $[UO_3(OH)_3]^{3-}$, **III**. One could argue that, if the proposed mechanism is correct, then this species should be visible in the experimental EXAFS spectra where it appears to be absent. Experimentally, the equilibrium between four- and five-coordinate species is not seen in the EXAFS at all but is only found in the ^{17}O NMR.[45] Therefore,

(89) Batista, E. R.; Martin, R. L.; Hay, P. J. *J. Chem. Phys.* **2004**, *121*, 11104.

whatever its particular mechanism, EXAFS cannot, apparently, be used to elucidate this exchange. This might simply be related to the time scales involved. Moreover, the interpretation of EXAFS spectra relies heavily on fitting and therefore on some model that the fitting procedure is based upon from the outset.[18] Indeed, Clark et al. as well as Wahlgren et al. state that the number of oxo ligands was *fixed* at a value of 2.0 for fitting their raw EXAFS data.[14,45] Consequently, one could speculate that the trioxide complex **III** was perhaps not seen because of a combination between the fast time scale of the exchange and the model used for fitting the EXAFS data. We also note the proven existence of the naked UO_3 molecule[90] that can be considered as a uranyl oxide (or an oxo complex of uranyl.) UO_3 has three partial triple bonds between the metal and the oxo ligands,[74] and it would in some ways be comparable to the newly proposed complex $[UO_3(OH)_3]^{3-}$ that also has calculated bond orders greater than 2 for each of the oxo ligands, Table 3.

Because proton shuttling is part of the hydrogen transfer steps (such as reaction 3a), quantum mechanical tunneling is non-negligible. One should therefore consider a tunneling-effect correction to all activation energies. In proton shuttling via the water molecule the imaginary frequencies are not significant enough, so the tunneling effect should be negligible (e.g., the transition state of reaction 3b, species **IX**, Table 1). On the other hand, high imaginary frequencies in transition states for proton shuttling through a hydrogen atom (e.g., the transition state of reaction 3a, species **VIII**, Table 1) can result in a considerable tunneling effect and might affect the barrier height. Modeling these effects is beyond the scope of the current study.

Conclusion

A three-step mechanism (Scheme 1) for the intramolecular oxygen exchange in uranyl hydroxide was suggested and explored computationally. Geometry optimizations of the reactants, transition states, and products in each step were carried out in the gas phase using DFT with the PBE and, in some cases, B3LYP functionals and in the condensed phase (solution) by DFT (PBE functional) and the COSMO model. Gas-phase frequency calculations were performed on the optimized gas-phase structures, in order to confirm the nature of the respective stationary point and to calculate free energies. From the energy calculations and barrier heights, it can be concluded that there is an equilibrium between the four-coordinated uranyl hydroxide and the anion, $[UO_3(OH)_3 \cdot H_2O]^{3-}$, which contributes to the interamolecular oxygen exchange with a favorable activation energy. We propose that the experimentally observed[45] equilibrium might not be between $[UO_2(OH)_4]^{2-}$ and $[UO_2(OH)_5]^{3-}$ but instead between $[UO_2(OH)_4]^{2-}$ and $[UO_3(OH)_3 \cdot H_2O]^{3-}$, because the barrier between $[UO_2(OH)_5]^{3-}$ and the latter is almost negligible.

The proposed mechanism is capable of explaining the experimentally observed, highly unusual facile oxygen ligand exchange in uranyl(VI) hydroxide[45] that, in itself, is remarkable because of the well-known stability and chemical inertness of the actinyl unit, for the hexavalent oxidation state in particular. The calculated activation energy for the rate-determining step in our mechanism ($\Delta H^{\ddagger} = 12.5$ kcal/mol in solution) compares favorably to the experimental value of 9.8 kcal/mol.[45] This gives strong support for our proposal in comparison to the alternative mechanisms proposed previously (concerted proton transfer[45] or a two-step mechanism involving intermediate "*cis*-uranyl" structures[44,50]) that have much higher activation energies. The principal reason for the difference lies in the extraordinary energetic stabilization of the linear uranyl moiety. This stabilization is maintained throughout our proposed mechanism but lost in the alternative cases.

We can conclude that the "riddle" of the intramolecular oxygen exchange in uranyl hydroxide, which has eluded a satisfactory explanation for some 12 years, might be solved. Our calculations do not support the proposal made by Szabo and Grenthe[55] that there is, in fact, no oxygen exchange occurring, and that the observed dynamic processes in alkaline solutions pertain to a tetrahydroxide/ pentahydroxide ($[UO_2(OH)_4]^{2-}/[UO_2(OH)_5]^{3-}$) equilibrium, eq 1, only. Indeed, we have shown that, once the pentahydroxide is reached, there is a facile pathway to complete the oxygen exchange.

Further study on this project could include frequency calculations in the condensed phase, studying the tunneling effect on barrier heights wherever a hydrogen transfer occurs with a significant imaginary frequency, and dynamical modeling of the system in the condensed phase, which might provide a more accurate representation of highly alkaline solutions. Extensions to the other early actinides (Np, Pu) and the pentavalent oxidation state are underway.

Acknowledgment. We are grateful to Dr. D. N. Laikov, Moscow/Stockholm, for making his Priroda code available to us. G.S. acknowledges N. B. Svenda, Winnipeg, for performing some auxiliary calculations for this project. Financial support from the Natural Sciences and Engineering Research Council of Canada is gratefully acknowledged.

Supporting Information Available: Complete citation for ref 69; Table S1 comparing energetics for reaction 3b using two different parameter settings for the COSMO solvation model; Table S2 containing the complete list of calculated vibrational frequencies and IR intensities for the proposed $[UO_3(OH)_3]^{3-}$ intermediate **III**. This material is available free of charge via the Internet at http://pubs.acs.org.

JA804742F

(90) Green, D. W.; Reedy, G. T.; Gabelnick, S. D. *J. Chem. Phys.* **1980**, *73*, 4207.